



HAL
open science

Formic Acid Electrooxidation on Palladium Nano-Layers Deposited onto Pt(111): Investigation of the Substrate Effect

Vanessa Oliveira, Y. Soldo, Edson Ticianelli, Marian Chatenet, Eric Sibert

► **To cite this version:**

Vanessa Oliveira, Y. Soldo, Edson Ticianelli, Marian Chatenet, Eric Sibert. Formic Acid Electrooxidation on Palladium Nano-Layers Deposited onto Pt(111): Investigation of the Substrate Effect. *Electrocatalysis*, 2023, 14 (4), pp.561-569. 10.1007/s12678-023-00816-z . hal-04034823

HAL Id: hal-04034823

<https://hal.univ-grenoble-alpes.fr/hal-04034823>

Submitted on 27 Jul 2023

HAL is a multi-disciplinary open access archive for the deposit and dissemination of scientific research documents, whether they are published or not. The documents may come from teaching and research institutions in France or abroad, or from public or private research centers.

L'archive ouverte pluridisciplinaire **HAL**, est destinée au dépôt et à la diffusion de documents scientifiques de niveau recherche, publiés ou non, émanant des établissements d'enseignement et de recherche français ou étrangers, des laboratoires publics ou privés.

1 **Formic acid electrooxidation on palladium nano-layers deposited**
2 **onto Pt(111): investigation of the substrate effect**

3 Vanessa L. Oliveira ^{1,2}, Yvonne Soldo-Olivier ^{1,3}, Edson A. Ticianelli ², Marian

4 Chatenet ¹, Eric Sibert ^{1,+}

5
6 ¹ Univ. Grenoble Alpes, Univ. Savoie Mont Blanc, CNRS, Grenoble INP (Institute of Engineering, Uni.
7 Grenoble Alpes), LEPMI, 38000 Grenoble, France

8 *Institute of Engineering and Management Univ. Grenoble Alpes

9 ² Instituto de Química de São Carlos, Universidade de São Paulo, Av. Trab. São-carlense 400, CP 780,
10 CEP 13560-970 São Carlos, SP, Brazil

11 ³ CNRS Université Grenoble Alpes, Institut Néel, 38042 Grenoble, France

12 + Corresponding author: eric.sibert@lepmi.grenoble-inp.fr

13 ORCID:

14 Yvonne Soldo-Olivier: 0000-0003-1624-0159

15 Edson A. Ticianelli: 0000-0003-3432-2799

16 Marian Chatenet: 0000-0002-9673-4775

17 Eric Sibert: 0000-0003-4084-1624

18 **Abstract**

19 The influence of Pd nano-layers electro-deposited onto Pt(111) single-crystal has
20 been systematically studied towards the formic acid electrochemical oxidation reaction
21 in H₂SO₄ and HClO₄. The studied Pd_xML/Pt(111) surfaces ($x = 1, 2, 5$ and 16
22 monolayers –ML-) are all more active than Pt(111) towards formic acid oxidation, even
23 if the activity is very sensitive to the Pd film thickness and morphology. In sulfate
24 solution, the competitive adsorption of long range ordered (bi)sulfate on the
25 pseudomorphic Pd terraces effectively hinders the formic acid oxidation only on the
26 thinnest films. We could observe the different role of the (bi)sulfate adsorption on the
27 first and on the following deposited Pd layers. The sulfate adsorption competitive role

28 rapidly fades away beyond about 5 ML of equivalent thickness, due to the surface
29 roughness increasing and terraces width diminishing.

30 In perchlorate media, anions do not adsorb competitively with formic acid
31 intermediates, allowing a larger activity of the formic acid oxidation up to about 5 ML.
32 At higher thicknesses, the difference in activity between the two electrolytic media is
33 reduced and it drops in both electrolytes close to 0.5 V vs. RHE, where Pd surface
34 oxides are formed.

35 Coupling the electrochemical results with the Pd layers structural description
36 previously obtained from *in situ* SXRD experiments, the outstanding activity of
37 Pd_{1ML}/Pt(111) observed in perchloric solution can be explained by the ligand effect of
38 the underlying platinum atoms on the first pseudomorphic Pd layer. This advantageous
39 effect is lost for Pd deposits thicker than 1 ML.

40

41 **Keywords:** Pt(111) single crystal; palladium layers; formic acid
42 electrooxidation; ligand and geometric effects.

43

44

45 **1. Introduction**

46 Small organic molecules, especially liquid C1-species, are attracting attention as
47 potential fuels for low temperature fuel cells, due to their propensity to be easily stored
48 and to the absence of C-C bonds that are difficult to break [1]. In this perspective,
49 methanol (CH₃OH), formaldehyde (HCHO) and formic acid (HCOOH) are among the
50 most investigated candidates. Despite an apparent simplicity, the complete oxidation of
51 these compounds involves several electron transfers that occur in multiple steps, leading
52 to a difficult overall optimization of appropriate electrocatalysts [2].

53 Typically, methanol electrooxidations on Pt in acidic media proceeds following
54 two main reaction paths. The indirect path starts with carbon atom dehydrogenation and
55 adsorption. It is followed by adsorbed CO formation that blocks active sites and results
56 in overall slow reaction kinetics. On the contrary, the direct path starts with oxygen
57 atom adsorption. Then, formaldehyde and formic acid can be produced as side products
58 and/or reaction intermediates before CO₂ is formed as a final product. So, improving the
59 activity of an electrode for formaldehyde and formic acid oxidation is not only
60 interesting by itself, but also for the methanol oxidation efficiency.

61 This two-paths mechanism is very common for the electrooxidation of small
62 organic molecules and also applies to formaldehyde and formic acid oxidation. The
63 selectivity between the two paths not only depends on the considered reaction, but is
64 always also governed by the surface structure of the electrode and the competitive anion
65 adsorption at its surface [3,4]. For the specific case of formic acid oxidation on
66 platinum, recent works highlight that a third path, with formate adsorption acting
67 mainly as poisoning specie, is possible [5].

68 The main approach to counteract the CO_{ads} formation and poisoning is to use a
69 bifunctional bimetallic electrocatalyst [6]. In this strategy, one of the two metals,

70 usually platinum, efficiently dehydrogenates/oxidizes the initial molecule, at least until
71 the formation of adsorbed CO_{ads}. In complement, the second one is a more oxophilic
72 metal that dissociates water molecule into OH_{ads}, which can react with CO_{ads} to produce
73 CO₂ in the well-known Langmuir-Hinshelwood reaction, thereby freeing active sites for
74 further activity.

75 While ruthenium is the most commonly-used second metal [6,7], palladium is
76 also gaining attention because (i) it is more oxophilic than platinum, (ii) has some
77 activity for the oxidation reactions at stake and (iii) can absorb hydrogen [8,9], playing a
78 (positive) role in the several dehydrogenation steps of C1-species oxidation.
79 Measurements on the three basal planes of Pd showed a high rate for formic acid
80 oxidation [10].

81 In the context of bimetallic catalysts, the use of well-ordered single crystals
82 surfaces modified by a foreign metallic atom deposition is not new in electrocatalysis.
83 Such modified ordered surfaces can provide original activities, typically due to strain or
84 ligand effects [11]. Moreover, their well-defined surface organization at the atomic level
85 with equivalent and uniformly-distributed active sites enables to (more) easily
86 understand complex electrochemical processes [1,8,9,12].

87 Several studies have been made on metallic single crystals modified by Pd
88 deposition towards the formic acid oxidation reaction. Kibler *et al.* [11] measured the
89 formic acid oxidation activity of a pseudomorphic atomic Pd surface layer on different
90 substrates (Au, Pt, Pd, Ir, Rh...) with (111) surface orientation in 0.1 mol L⁻¹ H₂SO₄ and
91 found that the activity is very sensitive to the nature of the substrate. More in detail, Pd
92 deposited on Pt(111) was found to exhibit a higher activity compared to all the studied
93 mono-metallic substrates or bulk Pd(111) surface. The authors suggest that, for all these
94 systems, the electronic modification of the Pd monolayer is essentially due to the

95 geometric factor, associated to the lateral strain of the Pd layer. This lattice mismatch
96 would induce a d-band shift, directly influencing bonding energies, as calculated by
97 Nørskov's group [13].

98 Llorca *et al.* [14] investigated this reaction on Pt(111) surface modified by Pd forced
99 deposition with coverages up to one atomic layer in 0.5 mol L⁻¹ H₂SO₄. As Pd addition
100 only induced marginal activity improvement, the authors suggested that CO poisoning,
101 although existing on free Pt(111), has limited extend on the overall activity; therefore
102 even if the Pd addition lowers poisoning, it cannot greatly change the activity that is
103 already good. In opposite, Baldauf *et al.* [15], using electrochemical deposition of Pd at
104 0.27 V *vs.* SCE on Pt(111) in 0.1 mol L⁻¹ H₂SO₄, observed changes in the activity for
105 coverage of 0.5 and 1 monolayer (ML). A new oxidation peak, reversible between
106 positive and negative scans of the cyclic voltammetry, appears and grows at lower
107 potential. It is associated to oxidation of formic acid through the direct path on Pd areas.
108 Nevertheless, the irreversible peaks associated to the oxidation through the indirect path
109 on Pt surface are still present at higher potential. Maximum oxidation currents are
110 slightly decreased compared to free Pt. For thicker deposits, from 2 to 5 ML as
111 equivalent thickness on Pt(111) (the equivalent thickness x ML is calculated assuming a
112 layer-by-layer growth mechanism with a two-electron-transfer process and one
113 deposited Pd atom per surface Pt atom), only a large reversible oxidation peak is
114 observed, suggesting that only the direct path remains on Pd. The activity is higher than
115 on free Pt, 0.5 and 1 ML Pd coverages.

116 Arenz *et al.* [9,16] studied the activity of a fraction up to 1 ML of Pd on Pt(111), as well
117 as a PtPd(111) bulk alloy in 0.1 mol L⁻¹ HClO₄. Both systems revealed a strong activity
118 enhancement compared to Pt(111), supporting the idea that the direct path is favored on
119 Pd, as shown by infrared measurements.

120 As first shown on polycrystalline Pd film deposited onto silicon with infrared
121 measurements, the activity of formic acid oxidation is also anion-sensitive: contrarily to
122 perchlorate, a competitive adsorption was observed between intermediate formate and
123 (bi-)sulfate [17].

124 Anion sensitivity was also seen for Pd films up to 2 ML on Pt(111) [1]. Deposits
125 were obtained after rapid immersion of the electrode in about 10^{-5} M $\text{Pd}(\text{NO}_3)_2$ solution
126 followed by reduction of Pd salts and deposition in hydrogen atmosphere. In aqueous
127 perchloric acid, adsorbed palladium promotes formic acid electrooxidation and a
128 maximum oxidation rate is found when a single Pd layer is deposited. In contrast,
129 voltammeteries recorded in aqueous sulphuric acid show a strong inhibition of this
130 reaction, which was attributed to extensive specific adsorption of (bi)sulphate anions,
131 competing with adsorption of formic acid molecules.

132 From the experimental point of view, Pd electrochemical deposit on Pt(111) in
133 acidic media can be tailored in a reproducible way at several well-defined thicknesses
134 when the first Pd layer is underpotentially deposited and following layers are obtained
135 scanning the potential very slowly ($v = 0.1 \text{ mV s}^{-1}$) down to a potential between UPD
136 and bulk deposition and holding it in-between [18].

137 The $\text{Pd}_{1\text{ML}}/\text{Pt}(111)$ deposit consists of a complete underpotentially deposited
138 (UPD) monolayer, pseudomorphic with the substrate (matching with the lattice of the
139 crystalline substrate) [19]. *In situ* surface X-Ray diffraction (SXRD) and *ex situ* AFM
140 experiments made by some of the authors of the present paper allowed the detailed
141 structural and morphological characterization of multilayered Pd nanofilms deposited in
142 PdCl_2 10^{-4} M + HCl $3 \cdot 10^{-3}$ + H_2SO_4 0.1 M solution [20,21]. For $\text{Pd}_{2\text{ML}}/\text{Pt}(111)$, the first
143 Pd layer is complete (UPD), the coverage of the second layer is about 80% and the
144 coverage of the third one is only 20%; for $\text{Pd}_{14\text{ML}}/\text{Pt}(111)$, the first ten Pd layers are

145 complete and the coverage progressively decreases until the twentieth layer, which is
146 nearly empty. The first ten Pd atomic planes are all pseudomorphic *i.e.* in-plane lattice
147 parameters of Pd layers are equal to that of the Pt(111) substrate, while the next Pd
148 layers are progressively relaxing to Pd bulk lattice parameters. These measurements
149 enable establishing a direct relationship between surface structure and electrochemical
150 characterization of the Pd/Pt(111) layers. Hence, the voltammetry in acidic media
151 allows determining the structure of the first deposited Pd layers onto Pt(111), without
152 resorting to physical characterization. *Ex situ* AFM images [18] show that up to 4 ML
153 the deposits present uniform flat zones, while roughness rapidly increases beyond this
154 thickness inducing the decrease of the terraces width.

155 The hydrogen insertion, obtained applying a sufficiently low potential to the
156 electrode, was also monitored by measuring the changes in the deposit lattice
157 parameters associated with hydride (Pd-H(β) phase) formation. No structural
158 modifications are observed for the first two Pd layer, both for thin or thicker deposits,
159 revealing that no hydride species are formed, not only between last the Pt and first Pd
160 layers, but also between the first and the second Pd atomic layers. Anisotropic
161 expansions in parallel and normal directions to the surface were recorded starting from
162 the third atomic Pd layer, corresponding to hydriding.

163 This detailed surface characterization coupled to the electrochemical study of the
164 Pd_{xML}/Pt(111) system towards formic acid oxidation reaction represents a unique
165 opportunity to correlate the surface structure to the reactivity. The present paper aims at
166 studying the influence of fine-tuned Pd/Pt(111) layers towards the electrooxidation of
167 formic acid. The study is performed in both H₂SO₄ and HClO₄ solutions, to specifically
168 address the mechanisms underlying the competitive adsorption between intermediate
169 formate species and (bi)sulfate, compared to perchlorate.

170

171 **2. Experimental details**

172 The working electrode (WE) was a Pt(111) single crystal cylinder with a 5 mm
173 diameter. The reference electrode (RE) was a saturated calomel electrode (SCE). It was
174 held in a separated compartment with a Luggin capillary connecting to the
175 electrochemical cell. The counter electrode was a Pt grid; a Pt sphere was used as the
176 auxiliary electrode to lower the electromagnetic noise. Detailed procedures are
177 described in Ref. [22]. An EG&G Princeton Applied Research, Model 273A
178 potentiostat/galvanostat with computer control was used for all the electrochemical
179 measurements.

180 For each experiment, the single crystal surface was cleaned and regenerated
181 using flame-annealing (butane + air). It was cooled in a reducing atmosphere (N₂/H₂
182 90:10) and finally put in contact with ultrapure water saturated with the same mixture,
183 as described previously [18,20]. A droplet of pure water was maintained at the electrode
184 surface to avoid contamination during all transfers between cooling glassware and cells
185 dedicated to electrochemical Pd deposition and characterization. Both cells were made
186 of Pyrex and double-walled designed to allow circulation of thermostated water for
187 temperature control at $25 \pm 1^\circ\text{C}$.

188 A cyclic voltamperogram in $0.1 \text{ mol L}^{-1} \text{ H}_2\text{SO}_4$ prepared from Merck sulfuric
189 acid (Suprapur, 96 %) in ultrapure water (Millipore Elix + Milli-Q gradient, $18.2 \text{ M}\Omega$
190 cm , $< 3 \text{ ppb}$ Total Organic Content) was recorded before each deposition experiment to
191 assess the Pt(111) surface quality and address the absence of contaminants in the system
192 [23–27].

193 A $0.1 \text{ mol L}^{-1} \text{ H}_2\text{SO}_4 + 3 \cdot 10^{-3} \text{ mol L}^{-1} \text{ HCl}$ (Merck, Suprapur 30%) + $10^{-4} \text{ mol L}^{-1}$
194 PdCl_2 (Alfa Aesar, 99%) solution was employed for palladium electrochemical

195 deposition. The Pt(111) electrode was first introduced at $E = 1.05$ V vs. RHE (at a
196 potential where no Pd deposition occurs) and then the potential was scanned negatively
197 to induce the Pd deposition. The single Pd atomic layer deposition ($x = 1$) was achieved
198 by underpotential deposition (UPD): the potential was simply scanned very slowly ($v =$
199 0.1 mV s⁻¹) to separate UPD and bulk deposition and held in-between. For thicker
200 deposits (Pd_{xML}/Pt(111) with $x = 2, 5$ and 16 ML), the Pd quantity was adjusted by
201 precisely measuring the coulometric charge assuming a layer-by-layer pseudomorphic
202 deposit (*i.e.* one palladium atom per each surface platinum atom and for each layer) and
203 two electrons transferred for each Pd atom [18,20,21]. Practically, the potential of the
204 Pt(111) electrode was scanned down ($v = 0.1$ mV s⁻¹) to Pd bulk and diffusion-limited
205 deposition ($E = 0.701$ V vs. RHE). The potential was then maintained at this value until
206 the required Pd quantity was obtained. After this, Pd_{xML}/Pt(111) electrodes were
207 emerged from the deposition solution, rinsed with ultra-pure water and transferred to the
208 characterization cell with pure acidic electrolyte (H₂SO₄ or and HClO₄) for control.

209 The electrooxidation of formic acid on the different Pt(111) and Pd_{xML}/Pt(111)
210 electrodes was investigated in 0.1 mol L⁻¹ H₂SO₄ + 0.1 mol L⁻¹ HCOOH and 0.1 mol L⁻¹
211 HClO₄ + 0.1 mol L⁻¹ HCOOH solutions.

212

213 **3. Results and discussion**

214 **3.1 Palladium deposition and electrochemical characterization in sulfuric acid**

215 As discussed in the introduction paragraph, electrochemical characterization in
216 sulfuric acid allows determining the atomic structure of the first Pd deposited layers.
217 Figure 1 exhibit representative cyclic voltamperograms (CVs) in aqueous sulfuric acid
218 (0.1 mol L⁻¹ H₂SO₄) of freshly-prepared Pd nanofilms and of the free Pt(111) surface,
219 also provided as benchmark. The Pt(111) surface (Figure 1, black curves) exhibits the

220 characteristic butterfly envelope, confirming the quality and cleanness of the Pt(111)
221 electrode surface [24–27]. Once Pd has been deposited, the corresponding
222 voltamperograms (Figure 1) are completely different, in accordance with the literature
223 [9,18,20,21,28–30].

224 For Pd_{1ML}/Pt(111), the platinum signature is no longer visible (Figure 1, red
225 curve), showing that the Pt(111) surface is fully covered by a complete UPD layer of
226 Pd. A new pair of sharp peaks appears around 0.21 V vs. RHE, associated to the
227 adsorption of electrolyte species on the first pseudomorphic Pd monolayer [22,30]. For
228 multilayered palladium deposits (Figure 1, blue, green and violet curves), a second pair
229 of broader peaks is present around 0.26 V vs. RHE, attributed to adsorption on second
230 and following Pd atomic layers [22,24]. For Pd_{2ML}/Pt(111), position and peaks
231 intensities indicate that the Pd film structure is very close to that revealed by *in situ*
232 SXRD experiments: a large part of the first Pd layer (close to 80%) is covered by the
233 second and following layers, while less than about 20% of the first Pd layer is still free.

234 Peaks corresponding to the first Pd layer are still partially present up to 5 ML,
235 showing that free first Pd layer regions, even if smaller and smaller in size, still remain
236 in contact with the electrolyte. Finally, the electrochemical response of Pd_{16ML}/Pt(111)
237 corresponds to a full covered first Pd layer.

238 Both pairs of peaks, associated with the first Pd layer and the “second and
239 following” layers, are associated with simultaneous hydrogen adsorption/desorption and
240 sulfate desorption/adsorption [12,30,31]. Adsorbed sulfates are forming an ordered
241 structure ($\sqrt{3}\times\sqrt{7}$)R19.1° on the Pd overlayers on Pt(111) [30], as on Pt(111) [32] and
242 bulk Pd(111) [33]. The sharpness of these adsorption peaks is associated with the
243 presence of a long-range order both on Pt(111) [26] and Pd(111) [33,34]. In opposite,
244 the broadening of the adsorption peaks observed with thicker Pd deposit is related to the

245 narrowing of flat Pd terraces and the reduction in size of long-range ordered sulfate
246 domains [35].

247 After experiments in formic acid, the electrodes were checked again in sulfuric
248 acidic solution, in order to probe possible surface irreversible modifications. The
249 adsorption/desorption charge is preserved, along with the signature of the palladium
250 layers (Supporting Information, Figure S1). Hence, this oxidation (formic acid is a mild
251 reducer) does not lead to irreversible structural modification of the Pd_xML/Pt(111)
252 surfaces, in opposite for instance to what was observed in presence of a strong reducer
253 like borohydrides [8].

254

255 **3.2 Formic acid electrooxidation on Pd_xML/Pt(111)**

256 Figure 2 shows a set of CVs during formic acid electrooxidation on
257 Pd_xML/Pt(111) and Pt(111), using 0.1 mol L⁻¹ H₂SO₄ (a) and 0.1 mol L⁻¹ HClO₄ (b)
258 electrolytes. All Pd_xML/Pt(111) surfaces exhibit higher activity than Pt(111) for this
259 reaction in both solutions. As already suggested in the literature, the lower activity of Pt
260 versus Pd is attributed to different overall reaction pathways for formic acid
261 electrooxidation on the two metals [1,14,16,36]. More specifically, “poisoning species”,
262 the most important being adsorbed CO, may hinder the electrooxidation of formic acid
263 on Pt, by blocking the active sites required for the adsorption of the HCOOH molecules
264 themselves, or for the H₂O adsorption and dissociation that are also needed for the
265 reaction [16,37]. In both media, CVs on Pt(111) are showing a strong difference
266 between the forward and backward scans, the second presenting larger currents. This is
267 due to the removal of CO at high potential, associated with the peak at $E = 0.75$ V vs.
268 RHE, providing a less blocked surface during the backward scan. In opposite, for Pd
269 surfaces, the forward and backward scans are much similar, with slightly less current for

270 the backward scan. This indicates that no consequent surface blocking by CO_{ads} is
271 occurring (if any), in accordance with the direct path mechanism.

272 Beyond the general benefit for formic acid oxidation adding Pd on Pt(111),
273 specific behaviors as a function of the equivalent Pd film thickness are observed in the
274 two electrolytes.

275 In presence of sulfate (Figure 2a), the onset of electrooxidation on Pt(111) is
276 measured at around $E = 0.3$ V vs. RHE, corresponding to the potential where a large
277 part of the surface is no more blocked by adsorption, as last vestiges of adsorbed
278 hydrogen are desorbing from the Pt(111) surface, and not yet majorly covered by
279 adsorbed sulfate species. When palladium is deposited on the electrode, the onset of
280 HCOOH electrooxidation, very close for all Pd modified samples, advantageously shifts
281 to more negative potentials (by *ca.* 0.2 V). Ahmed *et al.* [1] already observed this
282 behavior, and correlated it to the change in potential zero total charge values between
283 clean Pt(111) and Pd/Pt(111). Higher activity for Pd_{1ML}/Pt(111) versus Pt(111) was also
284 predicted using DFT calculations [38].

285 Concerning the formic acid electro-oxidation activity in sulfate electrolyte,
286 voltammeteries show a general increase of the formic oxidation current with thickness,
287 although the electrochemical response is characterized by a specific behavior as a
288 function of the number of deposited Pd layers. For Pd_{1ML}/Pt(111), there is a single
289 oxidation peak slightly above 0.2 V vs. RHE, at the same potential where the sharp
290 (bi)sulfate adsorption peak is observed in sulfuric acid solution (Figure 1): this
291 maximum is followed by a rapid decrease of the oxidation current. For Pd_{2ML}/Pt(111), at
292 this same potential, the curve presents only a shoulder and the current continues to
293 increase up to around 0.37 V vs. RHE: beyond this value the signal rapidly drops. The

294 current decrease is now in the potential region where (bi)sulfate adsorption takes place
295 on the free second and following Pd atomic layers.

296 Data of these two samples already allow a detailed description of the role of
297 (bi)sulfate adsorption as a competitive process hindering formic acid oxidation. For the
298 thinnest films, the responsible for the rapid oxidation current dropping is the long range
299 ordered competitive (bi)sulfate adsorption on the pseudomorphic terraces of the Pd free
300 surface. On Pd_{1ML}/Pt(111), it concerns the adsorption on the first Pd layer, at about 0.2 V
301 vs. RHE. On the other hand, this adsorption is no longer strong enough to effectively
302 stop the formic acid oxidation on Pd_{2ML}/Pt(111), where the uncovered part of the first
303 atomic Pd layer represents a minor part of the total electrode area; it only succeeds in
304 slowing down the reaction. For this thickness, it is the competitive (bi)sulfate long range
305 ordered adsorption on the terraces of the second and following Pd planes, at about 0.37
306 V vs. RHE, that effectively stops the oxidation reaction.

307 For Pd_{5ML}/Pt(111), only a barely visible shoulder is present at about 0.2 V vs.
308 RHE. In this sample, no significant influence of the competitive adsorption on the first
309 Pd layer is present, in agreement with the fact that at this thickness the largest part of
310 the first Pd layer is covered. The current maximum is still located in the potential region
311 of (bi)sulfate adsorption on the Pd layers terraces beyond the first Pd plane, close to
312 0.37 V vs. RHE, indicating that this competitive adsorption still plays a role in the
313 formic acid oxidation activity decrease. Nevertheless, it is less effective, as shown by
314 the less abrupt current drop after the maximum compared to the thinner samples. Only
315 beyond about 0.5 V HER the signal decrease accentuates, corresponding to the potential
316 region where Pd surface starts to oxidize.

317 For Pd_{16ML}/Pt(111), the current continuously increases up to about 0.5 V vs.
318 RHE (only a bump at about 0.37 V vs. RHE is visible). At this highest thickness, it

319 clearly appears that (bi)sulfate adsorption has a lost effectiveness in hindering formic
320 acid oxidation. This thickest deposit is also exhibiting the highest difference between
321 the positive and negative scans. The corresponding current excess during the positive
322 scan should be ascribed to the release of hydrogen absorbed in palladium at low
323 potential.

324 The comparison with pure Pd(111) surface in reference [39] is showing a
325 voltammetric profile similar to the present Pd_{5ML}/Pt(111), both in term of current and
326 potential at the current maximum. The morphological evolution of the Pd surface as a
327 function of the thickness as reported by Lebouin *et al.* [18] is particularly useful to
328 understand these observations. AFM images have shown that the Pd terraces width
329 largely decreases beyond about 4 ML as equivalent thickness, inducing the formation of
330 surface defaults which represent new adsorption sites. Our electrochemical results are in
331 complete agreement with this description: only when pseudomorphic Pd terraces width
332 is sufficiently large to allow long range ordered (bi)sulfate adsorption, anion adsorption
333 effectively inhibit formic oxidation. As for equivalent thickness increases beyond about
334 4-5 ML, the surface becomes quite rough and the terraces width shrinks, long range
335 ordered competitive adsorption is no more possible: as a result, formic acid oxidation
336 activity is larger and stops only at higher potential, where Pd surface oxidation process
337 begins. As a confirmation, the activity of pure Pd(111) in reference [39] is also lower
338 than that of Pd_{16ML}/Pt(111), although the lattice parameter of the Pd surface layer in
339 Pd_{16ML}/Pt(111) is relaxed to the one of Pd(111) [21]. The electronic effect of the
340 substrate should also be negligible for a such thick deposit. So, the only difference
341 between the two surfaces is their roughness, with wide flat areas for Pd(111) allowing
342 long range ordered (bi)sulfate, in opposite to narrow terraces for Pd_{16ML}/Pt(111) not
343 allowing it.

344 In presence of perchlorate (Figure 2b), the onsets of electrooxidation are very
345 similar to sulfuric media. It is around $E = 0.3$ V vs. RHE for Pt(111), and at $E = 0.2$ V
346 vs. RHE for Pd surfaces, *i.e.* at the end of hydrogen desorption on both surfaces. Then,
347 sweeping to higher potential values, Pd_{1ML}/Pt(111) exhibits the steepest current increase
348 and reaches the highest current maximum of all Pd deposits. Currents during positive
349 and negative scans are very similar. This is quite different from previous work from
350 Liang *et al.* [40]. They show a high irreversibility with low current at positive scan and
351 a peak at the beginning of negative scan, that should correspond to the oxidation of a
352 blocking/poisoning specie. One hypothesis would be that the higher formic acid
353 concentration (0.5 M instead of 0.1 M in the present work) is producing more poisoning
354 species, inducing a fast surface blocking. Uncompensated ohmic drop with high
355 currents measured in ref. [40] may also explain the observed shape with limited current
356 during the forward scan and the kind of switch at the beginning of the backward scan.

357 Pd_{2ML}/Pt(111) presents an intermediate case, with initial current increase smaller
358 than the Pd_{1ML}/Pt(111) electrode, but larger than thicker Pd deposits. In opposite, the
359 current maximum is the lowest of all Pd deposits. The 5 and 16 ML deposits are
360 showing similar behaviors with oxidation currents smaller than for the 1 and 2 ML until
361 $E = 0.4$ V vs. RHE. Like in sulfate media, the thickest Pd deposit is also showing the
362 highest current excess during the positive scan, attributed to hydrogen de-insertion. The
363 activity of Pd(111) in reference [39] is lower than for Pd_{1ML}/Pt(111), with a current
364 maximum around 10 mA.cm⁻² at 0.5 V vs. RHE, versus 10 mA.cm⁻² at 0.5 V vs. RHE
365 for the latter, this value being larger than for all other Pd deposits.

366 Figure 3 shows the comparison of formic acid activity in both media for the
367 same Pd layer thicknesses. Two different potential regions are present. Scanning from
368 low potential, the formic acid electro-oxidation activity firstly grows similarly in both

369 media. The reaction onset is not affected by the nature of the anions presents in
370 solution; also, current intensity behavior is very close. Contrarily, beyond about 0.25 V
371 vs. RHE, where (bi)sulfate adsorption is observed in the absence of formic acid,
372 oxidation currents behave differently: the activity is always larger with perchlorate than
373 with sulfate. Nevertheless, this deviation diminishes beyond about 5 ML, where,
374 contrarily to perchlorate, formic acid oxidation activity in presence of sulfate
375 significantly increases: finally, current intensities tend to converge at the highest
376 thickness. This observation is in complete agreement with the fact that only adsorbed
377 (bi)sulfate on the pseudomorphic terraces of the thinnest electrodes, where they form a
378 well-ordered structure, act as an effective barrier to formic acid oxidation. As thickness
379 increases, formic acid oxidation is less and less hindered by the (bi)sulfate adsorption.
380 Beyond about 4-5 ML, formic acid oxidation is stopped in both solutions (sulfate and
381 perchlorate) at higher potential, close to about 0.5 V vs. RHE, where Pd surfaces
382 deactivate owing to metal-oxides formation.

383 A very specific behavior is nevertheless observed for Pd_{1ML}/Pt(111) in
384 perchlorate, where the activity is the highest; it dramatically decreases at higher
385 thickness, already starting from two layers (Pd_{2ML}/Pt(111), Figure 3). Such behavior
386 was already observed by Ahmed *et al.* [1], but they had no structural description of the
387 electrode, preventing any understanding of the underlying mechanism. The activity is
388 also higher than the one of pure Pd(111) [39].

389 If such remarkable activity for Pd_{1ML}/Pt(111) were due to the larger creation of
390 poisoning species like CO_{ads} at higher thickness, where the abrupt increase of the
391 surface roughness compared to 1 ML induces a large number of under-coordinated
392 atoms at the edges [30], this process should also be observed in the voltamperometries.
393 Indeed, such a contamination is not shown by cyclic voltamperograms, that present

394 similar current intensities during positive and negative scans (contrarily to what is
395 observed for free Pt(111)). The higher activity of Pd_{1ML}/Pt(111) compared to thicker
396 samples must hence be ascribed to specific electrocatalytic properties of the first Pd
397 atomic layers, due to distinguished atomic and/or electronic structural properties.
398 Regarding the lattice parameters of the first and second plane atomic structure, SXRD
399 measurements have shown that they have the same values in both samples. All the Pd
400 atomic layers are pseudomorphic and none of the 1 ML or 2 ML deposits undergo
401 hydride formation (it can only occur between the second and the third atomic Pd layers,
402 but the occupation rate of this last layer can here be neglected) [20]. These arguments
403 clearly indicate that the specific activity of Pd_{1ML}/Pt(111) compared to Pd_{2ML}/Pt(111)
404 cannot be ascribed to geometric effects or to hydride formation. Electronic effect must
405 rather be considered. Indeed, the electronic interactions between the surface Pd atoms
406 and the underlying layers are different between the 1 ML and 2 ML deposits. Pd surface
407 atoms for Pd_{1ML}/Pt(111) are bounded to the underlying Pt atoms and have no Pd top
408 neighbors, while most of Pd surface atoms for Pd_{2ML}/Pt(111) are deposited onto Pd and
409 are not in contact with Pt atoms [20]. The ligand effect induced by the Pt substrate
410 seems thus to be the major responsible of the higher formic acid oxidation activity in
411 perchlorate media of Pd_{1ML}/Pt(111) compared to Pd_{2ML}/Pt(111). Chen *et al.* [41]
412 recently demonstrated that adsorption/desorption peaks observed at low potential on
413 Pd_{1ML}/Pt(111) in perchloric acid solution are not associated with hydrogen adsorption
414 only, but also to hydroxyl adsorption and, moving to higher potential, to perchlorate
415 specific adsorption. Although the presence of hydroxyl at such low potential (starting at
416 0.246 V vs. RHE) may explain the high activity toward formic acid electrooxidation, the
417 lack of similar experiments on thicker Pd deposits does not allow to draw any reliable
418 conclusion on this aspect.

419

420 **4. Conclusions**

421

422 The influence of Pd modified Pt(111) surfaces on the electrochemical oxidation
423 reaction of formic acid was investigated. We coupled our previous *in situ* SXRD
424 structural characterization of the Pd nanofilms with the voltammeteries recorded on
425 Pd_{xML}/Pt(111) ($x = 1, 2, 5, 16$) in H₂SO₄ and HClO₄ solutions supporting electrolyte.

426 The higher electrocatalytic activity of the Pd_{xML}/Pt(111) samples compared to
427 Pt(111) is confirmed in both acidic media, even if the effect is more pronounced in
428 HClO₄ compared to H₂SO₄. Our experiments show that on the thinnest films, up to
429 about 5 ML, the decay of formic acid is governed by the well-ordered structure of the
430 adsorbed (bi)sulfate of the electrode, acting as an effective barrier to formic acid
431 adsorption. We could detail the specific role of the competitive (bi)sulphate adsorption
432 on the first and on the following free pseudomorphic Pd terraces. Such effect diminishes
433 with thickness, as terraces width decreases with the roughening of the surface. Beyond
434 about 5 ML, decaying of formic acid activity is in both solutions close to 0.5 V vs.
435 RHE, due to the oxidation of the Pd surface, and activities in the two media tend to
436 converge for the highest thickness.

437 In perchlorate, the Pd_{1ML}/Pt(111) shows an outstanding activity. Thanks to the
438 detailed structural description of the surface Pd layers, we could demonstrate that, in the
439 absence of competing anion adsorption (which would be the case with (bi)sulfates), a
440 major role in formic acid oxidation activity is played by the ligand effect and not by
441 geometrical strains. This advantageous ligand effect is lost for thicker Pd deposits.

442

443 **5. Acknowledgments**

444 This work has been financially supported by the CAPES (project 728714-3).

445 **Conflict of Interest**

446 The authors declared that they have no conflict of interest.

447

448

449 **6. References**

- 450 [1] M. Ahmed, G.A. Attard, E. Wright, J. Sharman, Methanol and formic acid
451 electrooxidation on nafion modified Pd/Pt{111}: The role of anion specific
452 adsorption in electrocatalytic activity, *Catalysis Today*. 202 (2013) 128–134.
453 <https://doi.org/10.1016/j.cattod.2012.05.014>.
- 454 [2] T.H.M. Housmans, A.H. Wonders, M.T.M. Koper, Structure Sensitivity of
455 Methanol Electrooxidation Pathways on Platinum: An On-Line Electrochemical
456 Mass Spectrometry Study, *The Journal of Physical Chemistry B*. 110 (2006)
457 10021–10031. <https://doi.org/10.1021/jp055949s>.
- 458 [3] G. Samjeské, A. Miki, M. Osawa, Electrocatalytic Oxidation of Formaldehyde on
459 Platinum under Galvanostatic and Potential Sweep Conditions Studied by Time-
460 Resolved Surface-Enhanced Infrared Spectroscopy, *J. Phys. Chem. C*. 111 (2007)
461 15074–15083. <https://doi.org/10.1021/jp0743020>.
- 462 [4] G. Samjeské, A. Miki, S. Ye, M. Osawa, Mechanistic Study of Electrocatalytic
463 Oxidation of Formic Acid at Platinum in Acidic Solution by Time-Resolved
464 Surface-Enhanced Infrared Absorption Spectroscopy, *J. Phys. Chem. B*. 110
465 (2006) 16559–16566. <https://doi.org/10.1021/jp0618911>.
- 466 [5] E. Herrero, J.M. Feliu, Understanding formic acid oxidation mechanism on
467 platinum single crystal electrodes, *Current Opinion in Electrochemistry*. 9 (2018)
468 145–150. <https://doi.org/10.1016/j.coelec.2018.03.010>.
- 469 [6] M. Watanabe, S. Motoo, Electrocatalysis by ad-atoms. Part II. Enhancement of the
470 oxidation of methanol on platinum by ruthenium ad-atoms, *Journal of*
471 *Electroanalytical Chemistry*. 60 (1975) 267. [https://doi.org/10.1016/S0022-](https://doi.org/10.1016/S0022-0728(75)80261-0)
472 [0728\(75\)80261-0](https://doi.org/10.1016/S0022-0728(75)80261-0).
- 473 [7] M. Watanabe, S. Motoo, Electrocatalysis by ad-atoms. Part III. Enhancement of
474 the oxidation of carbone monoxide on platinum by ruthenium ad-atoms, *Journal of*
475 *Electroanalytical Chemistry*. 60 (1975) 275. [https://doi.org/10.1016/S0022-](https://doi.org/10.1016/S0022-0728(75)80262-2)
476 [0728\(75\)80262-2](https://doi.org/10.1016/S0022-0728(75)80262-2).
- 477 [8] V.L. Oliveira, E. Sibert, Y. Soldo-Olivier, E.A. Ticianelli, M. Chatenet,
478 Investigation of the electrochemical oxidation reaction of the borohydride anion in
479 palladium layers on Pt(111), *Electrochimica Acta*. 209 (2016) 360–368.
480 <https://doi.org/10.1016/j.electacta.2016.05.093>.
- 481 [9] M. Arenz, V.R. Stamenković, P.N. Ross Jr., N.M. Marković, Surface (electro-
482)chemistry on Pt(111) modified by a Pseudomorphic Pd monolayer, *Surface*
483 *Science*. 573 (2004) 57. <https://doi.org/10.1016/j.susc.2004.05.144>.
- 484 [10] N. Hoshi, K. Kida, M. Nakamura, M. Nakada, K. Osada, Structural Effects of
485 Electrochemical Oxidation of Formic Acid on Single Crystal Electrodes of

- 486 Palladium, *Journal of Physical Chemistry B*. 110 (2006) 12480.
487 <https://doi.org/10.1021/jp0608372>.
- 488 [11] L.A. Kibler, A.M. El-Aziz, R. Hoyer, D.M. Kolb, Tuning Reaction Rates by
489 Lateral Strain in a Palladium Monolayer, *Angewandte Chemie International*
490 *Edition*. 44 (2005) 2080. <https://doi.org/10.1002/anie.200462127>.
- 491 [12] B. Álvarez, V. Climent, A. Rodes, J.M. Feliu, Anion adsorption on Pt-Pd(111)
492 electrodes in sulphuric acid solution, *Journal of Electroanalytical Chemistry*. 497
493 (2001) 125. [https://doi.org/10.1016/S0022-0728\(00\)00466-6](https://doi.org/10.1016/S0022-0728(00)00466-6).
- 494 [13] A. Ruban, B. Hammer, P. Stoltze, H.L. Skriver, J.K. Nørskov, Surface electronic
495 structure and reactivity of transition and noble metals, *Journal of Molecular*
496 *Catalysis A*. 115 (1997) 421. [https://doi.org/10.1016/S1381-1169\(96\)00348-2](https://doi.org/10.1016/S1381-1169(96)00348-2).
- 497 [14] M.J. Llorca, J.M. Feliu, A. Aldaz, J. Clavilier, Formic acid oxidation on Pd +
498 Pt(100) and Pd + Pt(111) electrodes, *Journal of Electroanalytical Chemistry*. 376
499 (1994) 151. [https://doi.org/10.1016/0022-0728\(94\)03506-7](https://doi.org/10.1016/0022-0728(94)03506-7).
- 500 [15] M. Baldauf, D.M. Kolb, Formic Acid Oxidation on Ultrathin Pd Films on Au(hkl)
501 and Pt(hkl) Electrodes, *Journal of Physical Chemistry*. 100 (1996) 11375.
502 <https://doi.org/10.1021/jp952859m>.
- 503 [16] M. Arenz, V.R. Stamenković, T.J. Schmidt, K. Wandelt, P.N. Ross Jr., N.M.
504 Marković, The electro-oxidation of formic acid on Pt–Pd single crystal bimetallic
505 surfaces, *Physical Chemistry Chemical Physics*. 5 (2003) 4242.
506 <https://doi.org/10.1039/b306307k>.
- 507 [17] H. Miyake, T. Okada, G. Samjeské, M. Osawa, Formic acid electrooxidation on Pd
508 in acidic solutions studied by surface-enhanced infrared absorption spectroscopy,
509 *Phys. Chem. Chem. Phys.* 10 (2008) 3662. <https://doi.org/10.1039/b805955a>.
- 510 [18] C. Lebouin, Y. Soldo-Olivier, E. Sibert, P. Millet, M. Maret, R. Faure,
511 Electrochemically elaborated palladium nanofilms on Pt(1 1 1): Characterization
512 and hydrogen insertion study, *Journal of Electroanalytical Chemistry*. 626 (2009)
513 59–65. <https://doi.org/10.1016/j.jelechem.2008.11.005>.
- 514 [19] M.J. Ball, C.A. Lucas, N.M. Marković, V.R. Stamenković, P.N. Ross Jr., From
515 sub-monolayer to multilayer—an in situ X-ray diffraction study of the growth of
516 Pd films on Pt(111), *Surface Science*. 518 (2002) 201.
517 [https://doi.org/10.1016/S0039-6028\(02\)02122-2](https://doi.org/10.1016/S0039-6028(02)02122-2).
- 518 [20] C. Lebouin, Y. Soldo-Olivier, E. Sibert, M. De Santis, F. Maillard, R. Faure,
519 Evidence of the Substrate Effect in Hydrogen Electroinsertion into Palladium
520 Atomic Layers by Means of in Situ Surface X-ray Diffraction, *Langmuir*. 25
521 (2009) 4251–4255. <https://doi.org/10.1021/la803913e>.
- 522 [21] Y. Soldo-Olivier, M.C. Lafouresse, M. De Santis, C. Lebouin, M. De Boissieu, É.
523 Sibert, Hydrogen Electro-Insertion into Pd/Pt(111) Nanofilms: An in Situ Surface
524 X-ray Diffraction Study, *Journal of Physical Chemistry C*. 115 (2011) 12041–
525 12047. <https://doi.org/10.1021/jp201376d>.
- 526 [22] V.L. Oliveira, E. Sibert, Y. Soldo-Olivier, E.A. Ticianelli, M. Chatenet,
527 Borohydride electrooxidation reaction on Pt(111) and Pt(111) modified by a
528 pseudomorphic Pd monolayer, *Electrochimica Acta*. 190 (2016) 790–796.
529 <https://doi.org/10.1016/j.electacta.2016.01.013>.
- 530 [23] V. Briega-Martos, E. Herrero, J.M. Feliu, Borohydride electro-oxidation on Pt
531 single crystal electrodes, *Electrochemistry Communications*. 51 (2015) 144–147.
532 <https://doi.org/10.1016/j.elecom.2014.12.024>.
- 533 [24] M. Wakisaka, S. Morishima, Y. Hyuga, H. Uchida, M. Watanabe, Electrochemical
534 behavior of Pt-Co(111), (100) and (110) alloy single-crystal electrodes in 0.1 M

- 535 HClO₄ and 0.05 M H₂SO₄ solution as a function of Co content, *Electrochemistry*
536 *Communications*. 18 (2012) 55–57. <https://doi.org/10.1016/j.elecom.2012.02.008>.
- 537 [25] L. Blum, D.A. Huckaby, N. Marzari, R. Car, The electroreduction of hydrogen on
538 platinum(111) in acidic media, *Journal of Electroanalytical Chemistry*. 537 (2002)
539 7–19. [https://doi.org/10.1016/S0022-0728\(02\)01187-7](https://doi.org/10.1016/S0022-0728(02)01187-7).
- 540 [26] A.M. Funtikov, U. Stimming, R. Vogel, Anion adsorption from sulfuric acid
541 solutions on Pt(111) single crystal electrodes, *Journal of Electroanalytical*
542 *Chemistry*. 428 (1997) 147. [https://doi.org/10.1016/S0022-0728\(96\)05051-6](https://doi.org/10.1016/S0022-0728(96)05051-6).
- 543 [27] J.-F. Li, A. Rudnev, Y. Fu, N. Bodappa, T. Wandlowski, In Situ SHINERS at
544 Electrochemical Single-Crystal Electrode/Electrolyte Interfaces: Tuning
545 Preparation Strategies and Selected Applications, *ACS Nano*. 7 (2013) 8940–8952.
546 <https://doi.org/10.1021/nn403444j>.
- 547 [28] V. Climent, N.M. Marković, P.N. Ross Jr., Kinetics of oxygen reduction on an
548 epitaxial film of Palladium on Pt(111), *Journal of Physical Chemistry B*. 104
549 (2000) 3116. <https://doi.org/10.1021/jp993480t>.
- 550 [29] M. Arenz, V.R. Stamenković, T.J. Schmidt, K. Wandelt, P.N. Ross Jr., N.M.
551 Marković, CO adsorption and kinetics on well-characterized Pd films on Pt(111) in
552 alkaline solutions, *Surface Science*. 506 (2002) 287.
553 [https://doi.org/10.1016/S0039-6028\(02\)01423-1](https://doi.org/10.1016/S0039-6028(02)01423-1).
- 554 [30] R. Hoyer, L.A. Kibler, D.M. Kolb, The initial stages of palladium deposition onto
555 Pt(111), *Electrochimica Acta*. 49 (2003) 63–72.
556 <https://doi.org/10.1016/j.electacta.2003.07.008>.
- 557 [31] A.M. El-Aziz, R. Hoyer, L.A. Kibler, D.M. Kolb, Potential of zero free charge of
558 Pd overlayers on Pt(111), *Electrochimica Acta*. 51 (2006) 2518.
559 <https://doi.org/10.1016/j.electacta.2005.07.036>.
- 560 [32] A.M. Funtikov, U. Linke, U. Stimming, R. Vogel, An in-situ STM study of anion
561 adsorption on Pt(111) from sulfuric acid solutions, *Surface Science*. 324 (1995)
562 L343. [https://doi.org/10.1016/0039-6028\(94\)00774-8](https://doi.org/10.1016/0039-6028(94)00774-8).
- 563 [33] A.M. El-Aziz, L.A. Kibler, Influence of steps on the electrochemical oxidation of
564 CO adlayers on Pd(111) and on Pd films electrodeposited onto Au(111), *Journal of*
565 *Electroanalytical Chemistry*. 534 (2002) 107. [https://doi.org/10.1016/S0022-](https://doi.org/10.1016/S0022-0728(02)01150-6)
566 [0728\(02\)01150-6](https://doi.org/10.1016/S0022-0728(02)01150-6).
- 567 [34] N. Hoshi, K. Kagaya, Y. Hori, Voltammograms of the single-crystal electrodes of
568 palladium in aqueous sulfuric acid electrolyte: Pd(S)-[n(111)x(111)] and Pd(S)-
569 [n(100)x(111)], *Journal of Electroanalytical Chemistry*. 485 (2000) 55.
570 [https://doi.org/10.1016/S0022-0728\(00\)00098-X](https://doi.org/10.1016/S0022-0728(00)00098-X).
- 571 [35] B. Álvarez, J.M. Feliu, J. Clavilier, Long-range effects on palladium deposited on
572 Pt(111), *Electrochemistry Communications*. 4 (2002) 379.
573 [https://doi.org/10.1016/S1388-2481\(02\)00315-6](https://doi.org/10.1016/S1388-2481(02)00315-6).
- 574 [36] G.-Q. Lu, A. Crown, A. Wieckowski, Formic Acid Decomposition on
575 Polycrystalline Platinum and Palladized Platinum Electrodes, *The Journal of*
576 *Physical Chemistry B*. 103 (1999) 9700–9711. <https://doi.org/10.1021/jp992297x>.
- 577 [37] M. Arenz, V.R. Stamenković, T.J. Schmidt, K. Wandelt, P.N. Ross Jr., N.M.
578 Marković, The effect of specific chloride adsorption on the electrochemical
579 behavior of ultrathin Pd films deposited on Pt(111) in acid solution, *Surface*
580 *Science*. 523 (2003) 199. [https://doi.org/10.1016/S0039-6028\(02\)02456-1](https://doi.org/10.1016/S0039-6028(02)02456-1).
- 581 [38] A.O. Elnabawy, J.A. Herron, Z. Liang, R.R. Adzic, M. Mavrikakis, Formic Acid
582 Electrooxidation on Pt or Pd Monolayer on Transition-Metal Single Crystals: A
583 First-Principles Structure Sensitivity Analysis, *ACS Catal*. 11 (2021) 5294–5309.
584 <https://doi.org/10.1021/acscatal.1c00017>.

- 585 [39] J. Lei, Z. Wei, M. Xu, J. Wei, Y. Chen, S. Ye, Effect of sulfate adlayer on formic
586 acid oxidation on Pd(111) electrode, Chinese Journal of Chemical Physics. 32
587 (2019) 649–656. <https://doi.org/10.1063/1674-0068/cjcp1904079>.
- 588 [40] Z. Liang, L. Song, A.O. Elnabawy, N. Marinkovic, M. Mavrikakis, R.R. Adzic,
589 Platinum and Palladium Monolayer Electrocatalysts for Formic Acid Oxidation,
590 Top Catal. 63 (2020) 742–749. <https://doi.org/10.1007/s11244-020-01264-5>.
- 591 [41] X. Chen, L.P. Granda-Marulanda, I.T. McCrum, M.T.M. Koper, Adsorption
592 processes on a Pd monolayer-modified Pt(111) electrode, Chem. Sci. 11 (2020)
593 1703–1713. <https://doi.org/10.1039/C9SC05307G>.
- 594

Formic acid electrooxidation on palladium nano-layers deposited onto Pt(111): investigation of the substrate effect

Vanessa L. Oliveira ^{1,2}, Yvonne Soldo-Olivier ^{1,3}, Edson A. Ticianelli ², Marian

Chatenet ¹, Eric Sibert ^{1,+}

¹ *Univ. Grenoble Alpes, Univ. Savoie Mont Blanc, CNRS, Grenoble INP (Institute of Engineering, Uni. Grenoble Alpes), LEPMI, 38000 Grenoble, France*

**Institute of Engineering and Management Univ. Grenoble Alpes*

² *Instituto de Química de São Carlos, Universidade de São Paulo, Av. Trab. São-carlense 400, CP 780, CEP 13560-970 São Carlos, SP, Brazil*

³ *CNRS Université Grenoble Alpes, Institut Néel, 38042 Grenoble, France*

⁺ Corresponding author: eric.sibert@lepmi.grenoble-inp.fr

ORCID:

Yvonne Soldo-Olivier: 0000-0003-1624-0159

Edson A. Ticianelli: 0000-0003-3432-2799

Marian Chatenet: 0000-0002-9673-4775

Eric Sibert: 0000-0003-4084-1624

Figure Captions

Fig 1. Cyclic voltammograms for the Pt(111) and Pd_{xML}/Pt(111) electrodes in H₂SO₄ 0.1 mol L⁻¹, $\nu = 50 \text{ mV s}^{-1}$. Inset: same data, current scale multiplied by 4.

Fig 2. Cyclic voltammograms for the Pd_{xML}/Pt(111), $\nu = 50 \text{ mV s}^{-1}$ in (a) in H₂SO₄ 0.1 mol L⁻¹+ formic acid 0.1 mol L⁻¹, (b) HClO₄ 0.1 mol L⁻¹+ formic acid 0.1 mol L⁻¹.

Fig 3. Comparison of formic acid 0.1 mol L⁻¹ oxidation in H₂SO₄ 0.1 mol L⁻¹ (black curve) and HClO₄ 0.1 mol L⁻¹ (red curve) on Pd_{xML}/Pt(111) for different thicknesses. Same conditions as Figure 2. Inset: current maximum during positive scan from cyclic voltammograms.

Figure 1

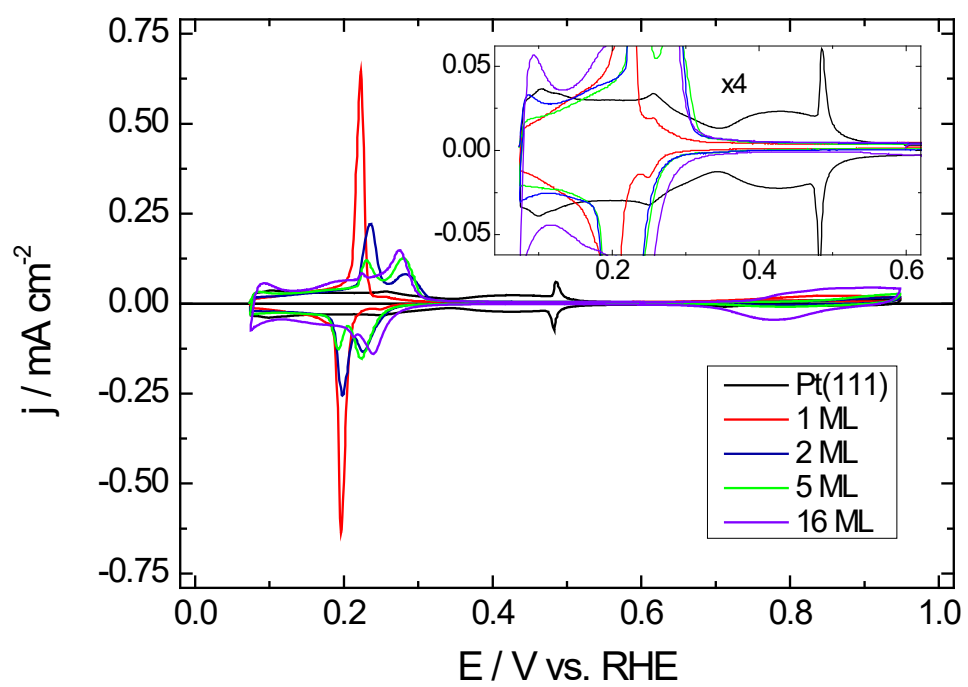


Figure 2

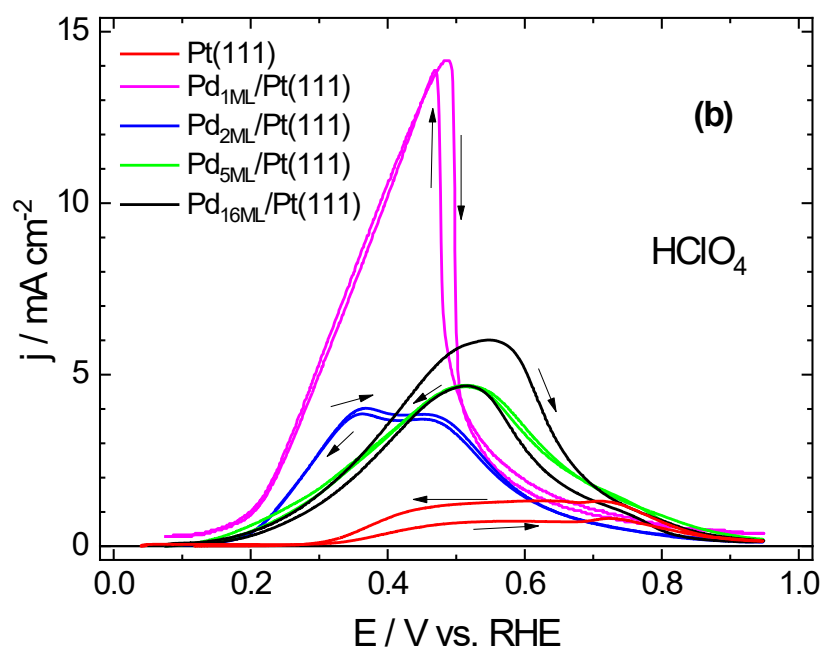
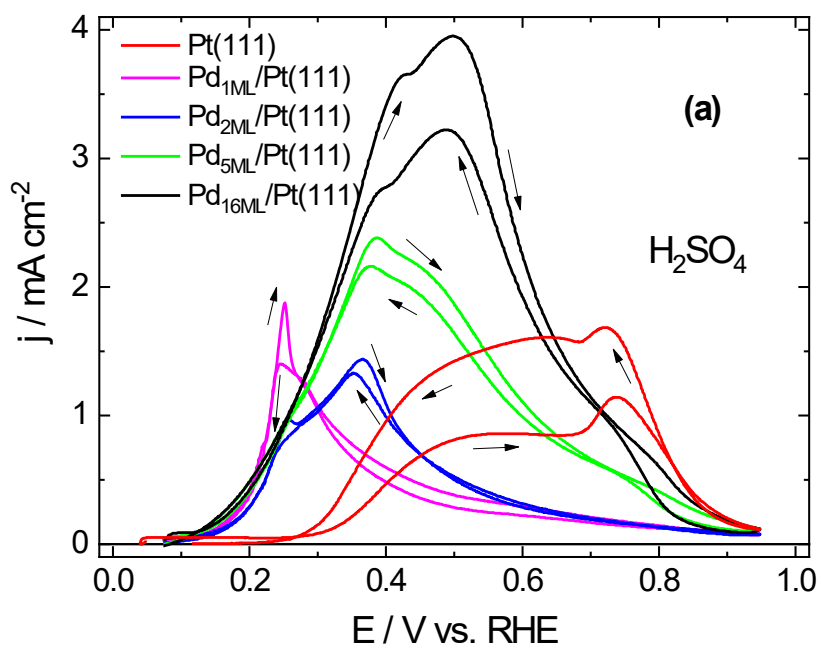
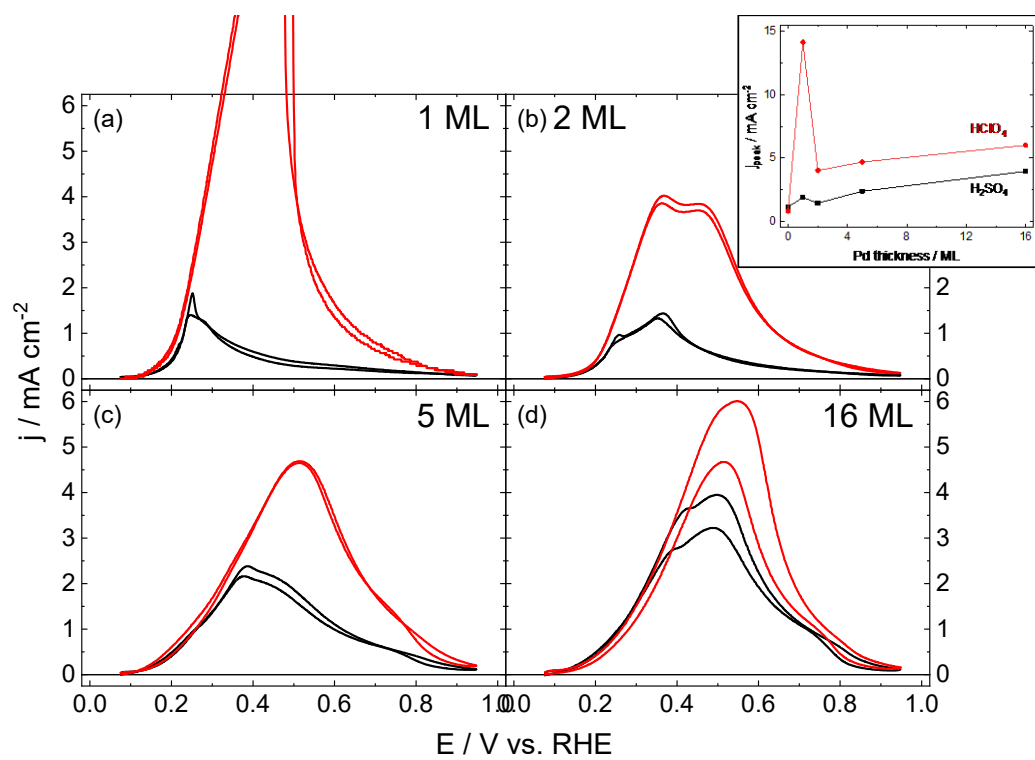


Figure 3



Supporting Information

Formic acid electrooxidation on palladium nano-layers deposited onto Pt(111): investigation of the substrate effect

Vanessa L. Oliveira ^{1,2}, Yvonne Soldo-Olivier ^{1,3}, Edson A. Ticianelli ², Marian

Chatenet ¹, Eric Sibert ^{1,+}

¹ Univ. Grenoble Alpes, Univ. Savoie Mont Blanc, CNRS, Grenoble INP (Institute of Engineering, Uni. Grenoble Alpes), LEPMI, 38000 Grenoble, France

*Institute of Engineering and Management Univ. Grenoble Alpes

² Instituto de Química de São Carlos, Universidade de São Paulo, Av. Trab. São-carlense 400, CP 780, CEP 13560-970 São Carlos, SP, Brazil

³ CNRS Université Grenoble Alpes, Institut Néel, 38042 Grenoble, France

⁺ Corresponding author: eric.sibert@lepmi.grenoble-inp.fr

ORCID:

Yvonne Soldo-Olivier: 0000-0003-1624-0159

Edson A. Ticianelli: 0000-0003-3432-2799

Marian Chatenet: 0000-0002-9673-4775

Eric Sibert: 0000-0003-4084-1624

1. Characterization after formic acid electrooxidation on Pd_xML/Pt(111)

The electrodes were characterized in supporting acidic medium also after the formic acid electrooxidation experiments, to provide insights about the definition/cleanness of the electrodes surface after the reactivity experiments. The voltammograms recorded after (blue curves) and before (black curves) formic acid electrooxidation (see Figure S1) are very similar: this demonstrates that the Pd_xML/Pt(111) surfaces do not undergo consequent irreversible modifications. The lower current densities measured are not surprising, considering that the several transfers undergone by the electrode between the various characterization cells may contaminate its surface.

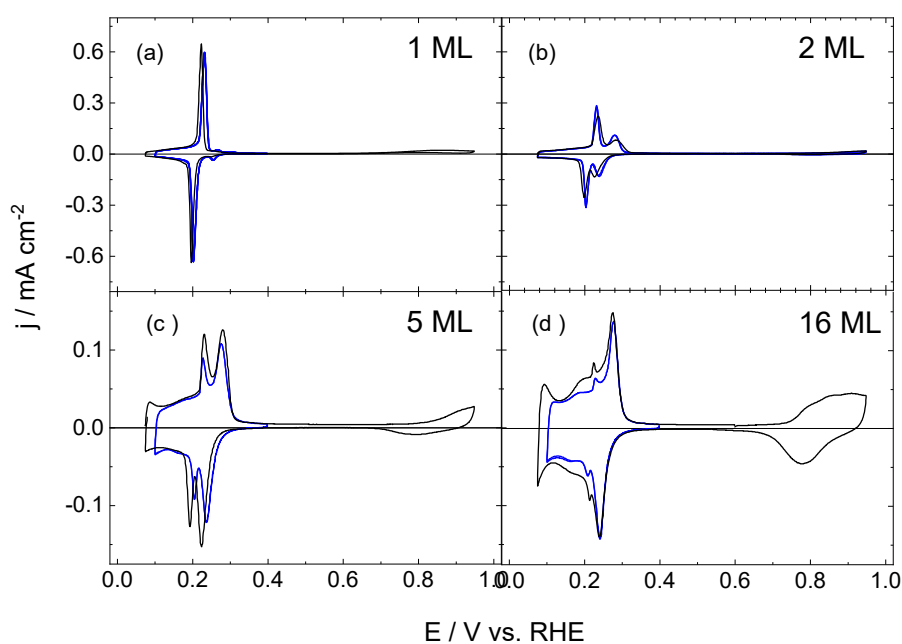


Figure S1. Cyclic voltammograms for Pd_xML/Pt(111) with (a) x = 1, (b) x = 2, (c) x = 5, (d) x = 16 in H₂SO₄ 0.1 mol L⁻¹, before (black line) and after (blue line) formic acid electrooxidation experiments.